

1 **Title:**

2 **A bacterial derived plant- mimicking cytokinin hormone regulates social behaviour in a**  
3 **rice pathogen**

4

5 **Authors**

6 Sohini Deb<sup>1</sup>, Chandan Kumar<sup>2</sup>, Rahul Kumar<sup>2</sup>, Amandeep Kaur<sup>3</sup>, Palash Ghosh<sup>1</sup>, Gopaljee  
7 Jha<sup>2</sup>, Prabhu B. Patil<sup>3</sup>, Subhadeep Chatterjee<sup>4</sup>, Hitendra K. Patel<sup>1</sup>, Ramesh V. Sonti<sup>1,2,5\*</sup>

8

9 **Affiliation**

10 <sup>1</sup>CSIR- Centre for Cellular and Molecular Biology (CSIR-CCMB), Hyderabad- 500007,  
11 India.

12 <sup>2</sup>National Institute of Plant Genome Research (NIPGR), New Delhi- 110067, India.

13 <sup>3</sup>CSIR - Institute of Microbial Technology (CSIR-IMTECH), Chandigarh- 160036, India.

14 <sup>4</sup>Centre for DNA Fingerprinting and Diagnostics (CDFD), Hyderabad- 500039, India.

15 <sup>5</sup>Current address: Indian Institute of Science Education and Research, Tirupati-517507, India

16 \*Corresponding author

17

18 **Contact Details**

19 Sohini Deb: [sohinideb.ccmb@gmail.com](mailto:sohinideb.ccmb@gmail.com) (ORCID: 0000-0002-4287-0886)

20 Ramesh V. Sonti: [sonti@ccmb.res.in](mailto:sonti@ccmb.res.in), Phone No.: +91- 40-27192577 (RVS)

21 (ORCID: 0000-0003-4845-0601)

22 **Word count:** 59,237 characters (with spaces)

23 **Keywords:** *Xanthomonas*/ type III effector/ biofilm/ cytokinin

## 24 **Abstract**

25 Many plant-associated bacteria produce plant- mimicking hormones which are involved in  
26 modulating host physiology. However, their function in modulating bacterial physiology has  
27 not been reported. Here we show that the XopQ protein, a type-III effector of the rice  
28 pathogen, *Xanthomonas oryzae* pv. *oryzae* (*Xoo*), is involved in cytokinin biosynthesis. *Xoo*  
29 produces and secretes an active form of cytokinin which enables the bacterium to maintain a  
30 planktonic lifestyle and promotes virulence. RNA-seq analysis indicates that the cytokinin  
31 produced by *Xoo* is required for the regulation of several genes which are involved in biofilm  
32 formation. We have also identified the *Xoo* isopentenyl transferase gene, which is involved in  
33 the cytokinin biosynthesis pathway and is required for maintaining planktonic behaviour and  
34 virulence. Furthermore, mutations in the predicted cytokinin receptor kinase (PcrK) and the  
35 downstream response regulator (PcrR) of *Xoo* phenocopy the cytokinin biosynthetic mutants,  
36 but are not complemented by supplementation with exogenous cytokinin. Cytokinin  
37 biosynthetic functions are encoded in a number of diverse bacterial genomes suggesting that  
38 cytokinin may be a widespread signalling molecule in the bacterial kingdom.

39

## 40 **Introduction**

41 Cytokinins are plant hormones that promote various aspects of plant growth, development  
42 and immunity (Osugi & Sakakibara, 2015). Several plant pathogenic bacteria such as  
43 *Rhodococcus fascians*, *Agrobacterium tumefaciens* and *A. rhizogenes* strains have been  
44 shown to produce cytokinins as part of their virulence repertoire in order to modulate host  
45 physiology (Pertry, Václavíková et al., 2009, Sardesai, Lee et al., 2013). Cytokinin

46 production by the plant growth promoting bacterium *Pseudomonas fluorescens* and the  
47 presence of intact plant cytokinin receptors has been shown to be necessary for biocontrol  
48 activity in *Arabidopsis thaliana* (Großkinsky, Tafner et al., 2016). *Mycobacterium*  
49 *tuberculosis* has also been shown to encode a phosphoribose-hydrolase that converts  
50 isopentenyl adenosine monophosphate (iPMP) to isopentenyl adenine (iP) and that it  
51 accumulates iP and 2-methylthio-iP in the culture medium (Samanovic, Tu et al., 2015).  
52 However, it is not known why *M. tuberculosis* produces cytokinin. *Corynebacterium*  
53 *glutamicum* encodes two proteins that can function as phosphoribose-hydrolases and a large  
54 number of prokaryotic organisms have been shown to have homologs of these enzymes  
55 (Samanovic et al., 2015, Seo & Kim, 2017). This suggests the intriguing possibility that  
56 cytokinins may be made by a number of bacteria and that these compounds may have a role  
57 in regulating bacterial physiology. Although it is well known that certain bacteria produce  
58 cytokinin to regulate host physiology, there is no evidence to date that endogenously  
59 produced cytokinin is used by bacteria to modulate their own physiology or cellular  
60 behaviour. Recently, a receptor for host produced cytokinin, named as Plant cytokinin  
61 receptor Kinase (PcrK), has been identified in the bacterium *Xanthomonas campestris* pv.  
62 *campestris* (*Xcc*), which can sense exogenously produced cytokinin. PcrK is a histidine  
63 kinase that is a part of the PcrK/PcrR two-component system, activation of which has been  
64 shown to enhance bacterial resistance to reactive oxygen species, produced as a part of the  
65 host defense response (Wang, Cheng et al., 2017).

66 The *Xanthomonas oryzae* pv. *oryzae* (*Xoo*) type III effector Xanthomonas outer protein Q  
67 (*XopQ*) is a homolog of the *Pseudomonas syringae* type III effector HopQ1, which appears  
68 to have phosphoribose-hydrolase activity (Hann, Dominguez-Ferreras et al., 2014). Here we  
69 report that *XopQ* is a phosphoribose-hydrolase which acts on the cytokinin precursor iPMP to  
70 produce cytokinin. Endogenous cytokinin production appears to control the ability of the

71 bacterium to remain in a planktonic state as the *xopQ*- mutant shows a tendency to form  
72 aggregates and enhanced biofilm formation. External supplementation of cytokinin to the  
73 *xopQ*- mutant restores its ability to remain in a planktonic mode as well as complements its  
74 virulence deficiency. We have further identified the *Xoo* isopentenyl transferase (*ipt*) gene  
75 which catalyzes an earlier step in the cytokinin biosynthetic pathway in *Xoo*. Mutation in the  
76 *ipt* gene predisposes the bacterium to form aggregates, enhances biofilm formation and  
77 reduces virulence; all of which can be restored by external supplementation of cytokinin.  
78 Thus, the *ipt*- mutant mimics the *xopQ*- mutant, consistent with the observation that they both  
79 affect cytokinin biosynthesis. RNA-seq analysis indicates differential expression of a number  
80 of genes in the *xopQ*- mutant that can affect biofilm formation.

81

## 82 **Results**

### 83 **The XopQ protein is a phosphoribose-hydrolase which produces cytokinin enabling the** 84 **planktonic growth of *X. oryzae* pv. *oryzae***

85 Earlier work had indicated that the aspartate residue at 116<sup>th</sup> position and tyrosine at 279<sup>th</sup>  
86 position are important for the phosphoribose-hydrolase activity of XopQ (Gupta, Nathawat et  
87 al., 2015). Hence, the purified recombinant proteins XopQ, XopQ D116A and XopQ Y279A  
88 were assayed for activity using the putative substrate isopentenyl adenosine monophosphate  
89 (iPMP). Activity of the wildtype XopQ protein, as well as mutant proteins, was found to  
90 increase with increasing substrate concentration but did not reach saturation. Activity was  
91 found to decrease at higher concentrations (Appendix Figure S1); possibly due to substrate  
92 inhibition. Hence, kinetic parameters were calculated using the substrate concentrations at  
93 which a linear increase in activity was observed. Similar  $K_m$  values for the wildtype and  
94 mutant indicated that mutations in the putative catalytic site of XopQ do not affect the

95 affinity of the XopQ enzyme for the substrate (Table 1, Appendix Figure S1). However, the  
96  $K_{cat}$  values indicated a strong activity of XopQ toward iPMP, as well as a significant  
97 reduction in the activity of the mutant proteins as compared to the wildtype XopQ protein.  
98 The lower  $K_{cat}/K_m$  value for the mutant proteins as compared to the wildtype XopQ protein  
99 suggested that the mutant proteins have less catalytic efficiency than the wildtype protein  
100 towards iPMP.

101 XopQ transcripts and protein were found to be expressed in the wildtype *Xoo* strain BXO43  
102 in laboratory PS media (Appendix Figure S2A, B). In order to determine if BXO43 produces  
103 cytokinin in laboratory cultures, we used LC/MS to estimate the amounts of the two  
104 cytokinins, isopentenyl adenine (iP) and trans-zeatin (tZ), in the cell pellet and culture  
105 supernatant of BXO43, mutant (*xopQ*-) and complement strains (*xopQ*-/pHM1, *xopQ*-  
106 /pHM1::*xopQ*, *xopQ*-/pHM1::*xopQ D116A* and *xopQ*-/pHM1::*xopQ Y279A*). Interestingly,  
107 the amount of iP produced by BXO43 in both cell pellet and supernatant was nearly 100- fold  
108 higher as compared to tZ (Fig 1A-D). As compared to BXO43, the *xopQ*- mutant produced  
109 significantly lesser amount of both iP as well as tZ, which could be complemented by  
110 introduction of the *xopQ* wildtype gene into the *xopQ*- strain through the pHM1 vector.  
111 Notably, the *xopQ D116A* and *xopQ Y279A* mutants failed to complement the reduction in  
112 cytokinin production of the *xopQ*- strain (Fig 1A-D).

113 Microscopic analysis revealed that *xopQ*- cells tend to form aggregates, in comparison to  
114 BXO43 cells, which remain dispersed (Fig 1E). We further went on to visualise the  
115 complement strains of *xopQ*-, i.e., *xopQ*-/pHM1, *xopQ*-/pHM1::*xopQ*, *xopQ*-/pHM1::*xopQ*  
116 *D116A* and *xopQ*-/pHM1::*xopQ Y279A*. The *xopQ*-/pHM1 strain formed aggregates, similar  
117 to the *xopQ*- mutant. However, complementation of the *xopQ*- cells with the wildtype *xopQ*  
118 gene restored a planktonic mode. Mutants in the *xopQ* gene which affected biochemical

119 activity and cytokinin production, namely the *xopQ*-/pHM1::*xopQ D116A* or *xopQ*-  
120 /pHM1::*xopQ Y279A* strains, formed aggregates similar to the *xopQ*- strain (Fig 1E).

121 We reasoned that the ability to form aggregates may result in a higher ability to form  
122 biofilms. To examine the role of *xopQ* in attachment and biofilm formation, we performed  
123 quantitative cell attachment and static biofilm assays using glass test tubes. The BXO43  
124 strain was seen to exhibit a minimal amount of biofilm formation as assayed after 4 days  
125 under biofilm formation conditions. However, the *xopQ*- strain formed significantly more  
126 biofilm, as visualized by staining with crystal violet (Fig 1F-H). This was also visualised by  
127 using the BXO43 or *xopQ*- strains expressing EGFP on a plasmid (Fig 1I, J). Introduction of  
128 the pHM1 empty vector into the *xopQ*- mutant did not alter the biofilm formation phenotype  
129 of the *xopQ*- strain. However, introduction of the wildtype *xopQ* gene on the complementing  
130 plasmid resulted in reduction in biofilm formation, a phenotype that was similar to that of  
131 BXO43. The biochemically inactive mutants *xopQ D116A* or *xopQ Y279A* were like the  
132 *xopQ*- mutant (Fig 1F-H).

### 133 **Supplementation with exogenous cytokinin converts a *xopQ*- mutant from biofilm to** 134 **planktonic phenotype and restores wildtype levels of virulence**

135 We examined whether addition of exogenous cytokinin would rescue the aggregation  
136 phenotype of the *xopQ*- cells. For this, the cytokinin iP was added to actively growing  
137 cultures of either BXO43 or the *xopQ*- mutant. Addition of iP could disperse the aggregates  
138 formed by cells of *xopQ*- (Fig 2A). Surprisingly, addition of cytokinin induced aggregate  
139 formation in the BXO43 strain. We also examined the ability of these strains to form biofilm.  
140 As described previously, the *xopQ*-, *xopQ*-/pHM1, *xopQ*-/pHM1::*xopQ D116A* and *xopQ*-  
141 /pHM1::*xopQ Y279A* strains formed more biofilm as compared to BXO43 or the *xopQ*-  
142 /pHM1::*xopQ* strains (Fig 1F-H). When iP was added, biofilm formation by the *xopQ*-, *xopQ*-

143 /pHM1, *xopQ*-/pHM1::*xopQ D116A* and *xopQ*-/pHM1::*xopQ Y279A* strains reduced  
144 significantly (Fig 2B-D). Addition of cytokinin induced higher biofilm formation in the  
145 BXO43 and *xopQ*-/pHM1::*xopQ* strains. Addition of iP to cultures of EGFP expressing  
146 derivatives of BXO43 and *xopQ*- strains led to reduced biofilm formation by the *xopQ*-  
147 strain, whereas it enhanced biofilm formation by BXO43 (Fig 2E-F).

148 We also examined if co-culture with the BXO43 strain would rescue the aggregate formation  
149 phenotype of the *xopQ*- strain. In order to distinguish the BXO43 and *xopQ*- strains, a  
150 *P<sub>lac</sub>*-mCherry plasmid was introduced into BXO43, while a EGFP plasmid was introduced  
151 into the *xopQ*- strain. When cultured individually, BXO43/mCherry cells were dispersed,  
152 whereas *xopQ*-/EGFP cells formed aggregates. On co-culturing these two strains, we  
153 observed that the *xopQ*-/EGFP strain no longer formed aggregates, and appeared to be  
154 dispersed (Fig 2G). These results suggest that, during co-culture, the cytokinin secreted by  
155 the BXO43 strain can rescue the aggregation phenotype of the *xopQ*- mutant.

156 The *xopQ*-, *xopQ D116A* and *xopQ Y279A* mutants of *Xoo* exhibit a virulence deficiency *in-*  
157 *planta* (Gupta et al., 2015). We determined whether external supplementation with active  
158 forms of cytokinin such as tZ or iP would restore the virulence deficiency of the *xopQ*-  
159 mutant. For this purpose, the BXO43, *xopQ*-, *xopQ*-/pHM1, *xopQ*-/pHM1::*xopQ*, *xopQ*-  
160 /pHM1::*xopQ D116A* and *xopQ*-/pHM1::*xopQ Y279A* strains were assayed for virulence on  
161 rice with or without addition of tZ or iP. In the absence of cytokinin, lesion lengths formed by  
162 either BXO43 or wildtype *xopQ* complemented strain were significantly longer than those  
163 obtained after infection with *xopQ*- or *xopQ*- expressing pHM1 vector alone, or pHM1  
164 expressing *xopQ D116A* or *xopQ Y279A* (Fig 2H). However, in the presence of tZ or iP,  
165 virulence of *xopQ*-, *xopQ*-/pHM1::*xopQ D116A* or *xopQ*-/pHM1::*xopQ Y279A* strains was  
166 restored to wildtype levels. These observations indicate that supplementation with exogenous  
167 cytokinin restores wildtype levels of virulence to the *xopQ*- mutant. Surprisingly, addition of

168 cytokinin in the presence of the wildtype copy of *xopQ* (i.e., BXO43 or *xopQ*-/pHM1::*xopQ*),  
169 resulted in reduced virulence of these strains, suggesting that an optimum level of cytokinin  
170 is necessary for complete virulence of *Xoo* (Fig 2H).

171 **The isopentenyl transferase gene is required for planktonic lifestyle and full virulence of**  
172 ***Xoo***

173 The isopentenyl transferase (*ipt*) gene encodes the committed step in the biosynthetic  
174 pathway of cytokinins. Putative IPT proteins were identified in *X. theicola*, *X. axonopodis*, *X.*  
175 *bromi*, *X. albilineans*, *X. translucens*, *X. oryzae* pv. *oryzae* PXO99a, *X. oryzae* pv. *oryzae*  
176 BXO1 and *X. oryzae* pv. *oryzicola* BLS256 by using *Agrobacterium tumefaciens* IPT protein  
177 as a query in NCBI GenBank. Alignment of the protein sequences revealed a high degree of  
178 conservation of this protein among these *Xanthomonas* species (Appendix Figure S3A).  
179 However, the *ipt* gene was absent in a few *Xanthomonas* species such as *X. campestris* pv.  
180 *vesicatoria* (*Xcv*) and *X. campestris* pv. *campestris* (*Xcc*) which infect dicotyledonous plants.  
181 Further bioinformatics analysis indicated that along with *ipt*, a 4777 bp region encompassing  
182 *ipt* is absent in both *Xcv* and *Xcc* (Fig 3A).

183 The *ipt* transcripts were found to be expressed in PS medium grown cultures of the BXO43  
184 strain (Appendix Figure S4). Analysis of the *ipt* gene in the *Xoo* genome indicated that it is  
185 conserved in nearly 100 sequenced Indian isolates of *Xoo* with 100% coverage and identity  
186 (unpublished observations, Prabhu B. Patil). Interestingly, the *ipt* gene has a G+C content of  
187 60%, which is significantly lesser than the average G+C content of *Xoo*, which is 64-65%,  
188 suggesting that *ipt* might have been acquired by horizontal gene transfer (Fig 3B). We also  
189 examined the codon usage pattern (CUP) of the *ipt* gene and observed that CUP of *ipt* as well  
190 of the 4777 bp region was significantly different from that of the housekeeping genes of *Xoo*  
191 and of the O-antigen biosynthetic gene cluster of *Xoo*, which has been earlier shown to have



192 the signature features of a genomic island (Patil & Sonti, 2004) (Fig 3C, D). Also, the  
193 presence of a IS630 family transposase and a tRNA-ser is consistent with this locus being a  
194 genomic island that has been acquired through horizontal gene transfer. This tRNA gene is  
195 present at the orthologous location in *Xcc* and *Xcv*, although the entire *ipt* genomic island is  
196 lacking in *Xcv* and *Xcc*. Bioinformatics analysis indicates that genes which encode homologs  
197 of the IPT protein are encoded in a number of bacteria (Appendix Figure S3B). Phylogenetic  
198 analyses of IPT proteins from diverse organisms has revealed the conservation of IPT  
199 proteins and their grouping into three clades (Appendix Figure S3B). The first clade  
200 contained only bacterial species with two subgroups of plant associated bacteria and soil  
201 bacteria; the second clade contained tRNA-type IPTs from all four groups, namely, Archaea,  
202 bacteria, fungi and plants, whereas the third group contained adenylate-type IPTs from fungi  
203 and plants.

204 Microscopic analysis of the *ipt*- strain revealed that these cells form aggregates, whereas cells  
205 of the wildtype (BXO43) remained dispersed (Fig 3E). Further, complementation of the *ipt*-  
206 mutant with the wildtype *ipt* gene reduced aggregate formation and restored the ability of the  
207 bacteria to grow in a planktonic mode. The *ipt*- strain also formed more biofilm as compared  
208 to BXO43 and complementation with the wildtype *ipt* gene restored the wildtype phenotype  
209 (Fig 3F-H). Microscopic analysis of EGFP expressing strains revealed that the *ipt*- strain  
210 formed a thicker biofilm as compared to BXO43 (Fig 3I-J). We further estimated the  
211 cytokinin content (tZ and iP) in both cell pellet as well as supernatant of the *ipt*- strain. As  
212 compared to BXO43, the *ipt*- strain showed a significant reduction in levels of both iP as well  
213 as tZ, which could be complemented by introduction of the wildtype *ipt* gene into the *ipt*-  
214 strain through the pHM1 vector (Fig 3K-N). The reduction in cytokinin levels, especially for  
215 iP, appears to be less than the reduction seen in the *xopQ*- mutant. This suggests that there

216 may be other substrates, besides those produced through action of IPT, on which XopQ can  
217 act to produce iP.

218 We then proceeded to examine the virulence of the *ipt-* strain. Leaves of 60- day old rice  
219 plants were inoculated with cultures of BXO43, *ipt-*, *ipt-*/pHM1 or *ipt-*/pHM1::*ipt*. The *ipt-*  
220 strain, as well as *ipt-* carrying the empty vector pHM1 showed a significant reduction in  
221 lesion length as compared to BXO43 at 14 days post inoculation. Introduction of the *ipt* gene  
222 in the *ipt-* mutant restored wildtype levels of virulence (Fig 3O-P).

### 223 **Supplementation of *ipt-* mutant with active cytokinin restores the wildtype phenotype**

224 In order to test if exogenous cytokinin addition would rescue the aggregate formation of an  
225 *ipt-* mutant, we added iP to actively growing cultures of the *ipt-* mutant. Addition of iP could  
226 disperse the aggregates formed by the *ipt-* mutant (Fig 4A). Cytokinin supplementation to the  
227 *ipt-* strain also led to reduced biofilm formation (Fig 4B-F). This was reflected in a lesser  
228 density of cells in culture in the *ipt-* strain as compared to BXO43 or *ipt-* + iP (Fig 4C). In  
229 order to check if the cytokinin secreted by BXO43 would rescue aggregate formation by *ipt-*,  
230 we went ahead to co- culture the BXO43/mCherry strain with the *ipt-*/EGFP strain. When  
231 cultured individually, BXO43/mCherry cells were dispersed, whereas *ipt-*/EGFP cells formed  
232 aggregates. On co- culturing these two strains, we observed that the *ipt-*/EGFP strain is  
233 dispersed and no longer formed aggregates (Fig 4G). This suggests that the cytokinin secreted  
234 by the BXO43 strain rescues the aggregation phenotype of the *ipt-* strain.

235 In order to determine if supplementation with iP would rescue the virulence deficiency of the  
236 *ipt-* strain, the strain was inoculated on rice leaves with or without injection of iP, 24h prior to  
237 infection. In the absence of iP, lesions caused by the *ipt-* strain were significantly shorter than  
238 those caused by the BXO43 strain. Supplementation with iP restored wildtype levels of  
239 virulence to the *ipt-* mutant (Fig 4H).

240 **The *pcrK/pcrR* genes are required for cytokinin sensing and virulence in *Xoo***

241 Recently, a cytokinin sensor named as Plant cytokinin receptor Kinase (PcrK), and its  
242 response regulator PcrR, have been identified in *Xcc* (Wang et al., 2017). Using them as a  
243 query, putative *pcrK* and *pcrR* genes were identified in the genome of *Xoo*. Microscopic  
244 analysis of the *pcrK*- and *pcrR*- strains revealed that these cells form aggregates, as compared  
245 to cells of BXO43, which remained dispersed (Fig 5A). The *pcrK*- and *pcrR*- strains also  
246 formed more biofilm as compared to BXO43 (Fig 5B-D). In order to test if exogenous  
247 cytokinin addition would rescue the aggregate formation of the *pcrK*- and *pcrR*- mutants, we  
248 added iP to actively growing cultures of the *pcrK*- and *pcrR*- mutants. However, addition of  
249 iP could neither disperse aggregate formation by cells of *pcrK*- and *pcrR*- mutants (Fig 5E)  
250 nor rescue the increased biofilm formation phenotype of these strains (Fig 5F-I). In order to  
251 check if the cytokinin secreted by BXO43 would rescue aggregate formation by *pcrK*- and  
252 *pcrR*-, we co- cultured the BXO43/mCherry strain with either the *pcrK*-EGFP or the *pcrR*-  
253 /EGFP strains. When cultured individually, BXO43/mCherry cells were dispersed, whereas  
254 the *pcrK*-EGFP and *pcrR*-EGFP cells formed aggregates. On co- culturing these two mutant  
255 strains with BXO43/mCherry, we observed that the strains still showed aggregate formation  
256 (Fig 5J). This suggests that the cytokinin secreted by the BXO43 strain is unable to rescue the  
257 aggregation phenotype of the *pcrK*-EGFP and *pcrR*-EGFP strains.

258 We then proceeded to examine the virulence of the *pcrK*- and *pcrR*- strains. Leaves of 60-  
259 day old rice plants were inoculated with cultures of BXO43, *pcrK*- or *pcrR*-. As compared to  
260 BXO43, both the *pcrK*- and *pcrR*- strains showed a significant reduction in lesion length as  
261 compared to BXO43 at 14 days post inoculation, indicating that cytokinin sensing is  
262 important for complete virulence of *Xoo* (Fig 5K, L).

263 **XopQ regulates the biofilm to planktonic lifestyle switch in *Xoo***

264 In order to gain a greater understanding of the regulatory role of XopQ, RNA- sequencing  
265 (RNA-seq) analysis was performed to assess differential gene expression between BXO43  
266 and the *xopQ*- strain. In the absence of XopQ, there were a total of 757 differential expressed  
267 genes (DEGs), of which 328 were down-regulated and 459 were up-regulated. Differential  
268 expression of 10 such genes was validated by RT-qPCR (Appendix Table S4, Appendix  
269 Figure S5A, b). GO analysis revealed the abundance of bacterial motility, bacterial flagellar  
270 assembly and protein transport related functional categories (Appendix Figure S5C). Further,  
271 KEGG pathway analysis using the genome annotation of *Xoo* strain BXO1 (Midha, Bansal et  
272 al., 2017), revealed “biofilm formation”, “bacterial chemotaxis” and “flagellar assembly”  
273 related pathways to be upregulated in the *xopQ*- mutant. Upregulation of the pathway for  
274 biofilm formation was consistent with our observation that the *xopQ*- mutant forms more  
275 biofilm. In this regard, upregulation of *cheA*, *cheB*, *cheV*, *cheW*, *cheY* and *mcp* genes was  
276 noteworthy in the *xopQ*- mutant. Silencing of *mcp*, *cheB*, and *cheV* by RNAi has earlier been  
277 shown to lead to deficiencies in adhesion, chemotaxis, flagellar assembly and motility  
278 (Huang, Wang et al., 2017). This may lead to increased cellular adhesion, similar to what is  
279 observed in the *xopQ*- mutant. Furthermore, the KEGG analysis revealed components of type  
280 IV secretion system to be up-regulated in the *xopQ*- mutant and previous results indicate this  
281 secretion system is involved in promoting biofilm formation (Cenens, Andrade et al., 2020,  
282 Elhenawy, Hordienko et al., 2021, Seifert, 2017). Notably, components of the type III  
283 secretion apparatus were amongst down-regulated pathways in the *xopQ*- mutant (Appendix  
284 Table S5). We observed the reduced expression of protein components of the type III  
285 secretion system (T3SS) and multiple type III effectors in the *xopQ*- mutant, which could be  
286 rescued by the addition of iP (Appendix Figure S5D). This suggests that expression of these  
287 proteins is regulated by cytokinin and may explain the reduced virulence of the *xopQ*-

288 mutant. Expression of the T3SS has previously been shown to be repressed in biofilm-  
289 growing bacteria (Kuchma, Connolly et al., 2005).

290

## 291 **Discussion**

292 The production of the phytohormone cytokinin by various phytopathogenic bacteria to  
293 modulate host physiology and virulence is well known. However, there are no reported  
294 examples of bacterial cytokinin production modulating bacterial physiology or social  
295 behaviour. Here we report the production of cytokinin by the rice pathogen *Xoo* and present  
296 evidence that cytokinin production controls the switch between biofilm and planktonic states.  
297 An important initial step in colonization during bacterial infection is adhesion. In  
298 *Xanthomonas*, this has been shown to involve the expression of multiple virulence factors,  
299 which includes surface appendages such as flagellum and type IV pili, which are required for  
300 the colonization of host tissues (Huang et al., 2017, Qi, Huang et al., 2020). However, post-  
301 colonisation spread in the host plant requires a switch from biofilm to planktonic lifestyle for  
302 an effective spread *in-planta* (Appendix Figure S6). We propose that bacterial cytokinin  
303 regulates this switch in *Xoo* and promotes virulence.

304 Our results indicate that the *Xoo* type III effector XopQ is a phosphoribose-hydrolase and can  
305 convert iPMP to iP. XopQ and its orthologs have earlier been shown to be required for full  
306 virulence, and immune response modulation (Deb, Ghosh et al., 2020, Deb, Gupta et al.,  
307 2019, Giska, Lichocka et al., 2013, Gupta et al., 2015, Li, Chiang et al., 2013, Li, Yadeta et  
308 al., 2013, Teper, Salomon et al., 2014) (Appendix Figure S7). *Arabidopsis* transgenic plants  
309 expressing the *Pseudomonas* ortholog HopQ1 show suppression of Flg22-induced defense  
310 responses by attenuating flagellin receptor FLS2 expression in a cytokinin dependent manner  
311 (Hann et al., 2014). HopQ1 has been predicted to catalyse the last step in the production of

312 cytokinin, converting iPMP to the active cytokinin iP. In flowering plants, this step is  
313 catalysed by the cytokinin riboside 5'-monophosphate phosphoribohydrolase (LONELY  
314 GUY/ LOG) class of enzymes, which catalyze the formation of active cytokinin species from  
315 cytokinin ribosides (Kurakawa, Ueda et al., 2007). Recently, the only homolog of this  
316 enzyme from the unicellular green microalga *Chlorella* was shown to be a cytokinin-  
317 activating enzyme (Nayar, 2021).

318 The *Xoo* genome encodes a homolog of the IPT protein that is predicted to catalyze the  
319 committed step in cytokinin production. The *ipt* mutant is defective in cytokinin production  
320 as well as virulence and exhibits the same aggregation phenotype as the *xopQ*- mutant. These  
321 phenotypes are reversed by cytokinin supplementation. The estimation of cytokinin levels in  
322 *Xoo* revealed that the levels of iP was almost 100-fold more as compared to trans-zeatin (tZ).  
323 This is similar to what is observed in the cyanobacterium *Nostoc* (Frébortová, Greplová et al.,  
324 2015). *Nostoc* was also shown to have a complete cytokinin synthesis machinery, with a  
325 conserved isopentenyl transferase (IPT) protein and a cytokinin dehydrogenase (CKX)  
326 protein (Frébortová et al., 2015). Our transcriptome data indicates upregulation of the biofilm  
327 formation pathway as well as type IV bacterial secretion pathway in the *xopQ*- mutant as  
328 compared to BXO43. This might explain why the *xopQ*- mutant has an enhanced biofilm  
329 formation phenotype. A reduced expression of the type III secretion system, and multiple  
330 type III effectors is observed in the *xopQ*- mutant, suggesting that this could also lead to the  
331 reduced virulence of the *xopQ*- mutant. How might cytokinin be sensed by *Xoo*? Our studies  
332 suggest that mutations in either the predicted cytokinin receptor kinase (PcrK) or the response  
333 regulator PcrR of *Xoo* results in phenotypes that are akin to those of the *xopQ*- and *ipt*-  
334 mutants, suggesting that these proteins could be involved in cytokinin sensing by *Xoo* (Fig 5).  
335 Interestingly, the *ipt* gene and the 4777 bp region encompassing it are present in some but not  
336 all members of the genus. The presence of this gene cluster in some but not all *Xanthomonas*

337 species, the atypical codon usage pattern and the presence of a tRNA gene near the *ipt* cluster  
338 are consistent with the possibility that this gene cluster may have been inherited by horizontal  
339 gene transfer. A large number of bacteria have genes that are predicted to encode  
340 phosphoribose-hydrolase and isopentenyl transferase activities and a few have been shown to  
341 produce cytokinin (Samanovic et al., 2015, Seo & Kim, 2017). Thus, cytokinins are produced  
342 by a number of different bacteria. Our results demonstrate for the first time that endogenously  
343 produced cytokinin regulates physiological activities in bacteria. We postulate that cytokinin  
344 may be an important signalling molecule in a number of bacterial species. Furthermore, we  
345 suggest that the origins of cytokinin as a signalling molecule may be rooted in bacteria and  
346 that this role may have been subsequently elaborated upon in the plant kingdom.

347

## 348 **Materials and methods**

### 349 **Bacterial strains, plasmids, media and growth conditions**

350 The plasmids and bacterial strains used in this study are listed in Appendix Table S1 and  
351 Appendix Table S2 respectively. The *Xoo* strains were grown at 28 °C in peptone- sucrose  
352 (PS) media (Daniels et al., 1984). *Escherichia coli* strains were grown in Luria–Bertani (LB)  
353 medium at 37 °C. Antibiotics were added at the following concentrations in the media:  
354 rifampicin: 50 µg/mL; kanamycin: 50 µg/mL (*E. coli*), 15 µg/mL (*Xoo*); spectinomycin: 50  
355 µg/mL; gentamicin: 10 µg/mL.

### 356 **Microscopy**

357 To monitor cell morphology, overnight grown *Xoo* strains were harvested, concentrated and  
358 immobilized on a thin agarose pad of 2 % agarose and visualized under a Zeiss AxioImager  
359 microscope in DIC (Nomarski optics) mode. For co-culturing of strains, the overnight grown  
360 cultures (BXO43/mCherry and *xopQ*-/EGFP or *ipt*-/EGFP) were adjusted to equal cell

361 density, mixed and incubated at 28 °C for 4 h. For assays involving the addition of cytokinin,  
362 the overnight grown cultures were adjusted to equal cell density, and 20 nM iP was added to  
363 the secondary culture, which was grown at 28 °C for 24 h.

#### 364 **Confocal microscopy for biofilm visualisation**

365 To monitor biofilm formed by the *Xoo* strains, BXO43, *xopQ*- and *ipt*- strains were  
366 transformed with the EGFP- expressing plasmid pMP2464 (Appendix Table S1) (Stuurman,  
367 Pacios Bras et al., 2000), grown overnight at 28 °C and normalized to an O.D.<sub>600</sub> of 0.1. 15  
368 ml of the culture was taken in a 50 ml tube and a sterilised glass slide was introduced into it.  
369 This was kept stationary at 28 °C for 72 h. To evaluate biofilm formation, the slide was  
370 washed gently with MQ water to remove loosely adhering cells, and further fluorescent Z-  
371 stacked images were acquired of 0.38 µm to measure overall attachment and biofilm levels at  
372 the air- culture interface on the slide at 63X in a LSM880 confocal microscope. The Zen  
373 software was used to plot the GFP signal intensity profile for the Z-stacked images for  
374 biofilm thickness and Imaris software was used to process the images for surface 3D  
375 visualisation.

#### 376 **Quantitative cell attachment and static biofilm assays**

377 *In- vitro* biofilm formation was visualised and quantified. The strains were grown overnight  
378 at 28 °C and normalized to an O.D.<sub>600</sub> of 0.1 in PS media in glass tubes. This was incubated  
379 for 4 days at 28 °C without shaking. In order to quantify cells remaining in planktonic state,  
380 the culture was decanted carefully, and OD<sub>600</sub> reading was taken. The glass tube was washed  
381 three times with MQ gently to remove any non- adhering cells. The resultant biofilm was  
382 further stained with a 0.1% crystal violet solution, at room-temperature for 30 min. Following  
383 this, the stain was removed, excess stain washed off, and the tubes were imaged. For  
384 quantification of biofilm, the crystal violet stain was solubilized using a combination of 40 %



385 methanol and 10 % glacial acetic acid. Data was collected in the form of the O.D.<sub>570</sub> of the  
386 elution.

### 387 ***In- vitro* enzyme assay**

388 Phosphoribose-hydrolase activity for XopQ and its mutants was performed with purified  
389 proteins by using the substrate N6-(2-isopentenyl) adenine-9-ribose-5'-monophosphate  
390 (OlChemIm Ltd., Olomouc, Czech Republic; Cat. No: 001 5043) as described previously  
391 (Hann et al., 2014) with modifications. The assay mixture contained purified 1pM enzyme  
392 supplemented with various concentrations of the substrate, in a 200µl reaction buffer (50mM  
393 HEPES, 100mM NaCl, 10mM imidazole pH 7.0 containing 1mM dithiothreitol and 5mM  
394 CaCl<sub>2</sub>). The reaction was performed for 5 s at 37 °C, and terminated by the addition of NaOH  
395 to a final concentration of 0.1 N. Product formation was measured as change in absorption at  
396 280 nm. 6-(γ,γ-dimethylallylamino) purine (Sigma; Cat. No: D5912-5G) was used for  
397 calculation of standard curve.

### 398 **Virulence assays**

399 60-day-old rice plants of the susceptible rice 'Taichung Native' (TN-1) were used for assays  
400 for virulence. *Xoo* strains were grown to saturation and inoculated by dipping scissors into  
401 bacterial cultures of O.D.<sub>600</sub>=1 and clipping the tips of rice leaves. Lesion lengths were  
402 measured at 14 days after inoculation and expressed as the mean lesion length with standard  
403 deviation.

404 In order to study the effect of exogenous supplementation of cytokinin, 10nM isopentenyl  
405 adenine or trans-zeatin was injected into the midvein of 60-day old TN-1 rice leaves. 24 h  
406 post injection, pin- prick inoculation of the respective *Xoo* strains was done 1 cm above the  
407 point of injection. Lesion lengths were measured at 14 days after inoculation and expressed  
408 as the mean lesion length with standard deviation.

## 409 **Estimation of cytokinin**

410 Bacterial strains were grown to saturation, cell pellet and supernatant were separated and  
411 lyophilised, and cytokinin was extracted by methanol/formic acid/water (15/0.1/4 v/v/v),  
412 using the internal standards *trans*-[<sup>2</sup>H<sub>5</sub>]zeatin and [<sup>2</sup>H<sub>6</sub>]isopentenyl adenine (OIChemIm Ltd.,  
413 Olomouc, Czech Republic). The extracts were purified using an C<sub>18</sub> RP SPE column and  
414 analysed using a 6500+ Qtrap system coupled with ultra-performance liquid chromatography  
415 using a Zorbax C18 column.

## 416 **Codon Usage Pattern**

417 Codon Usage Pattern (CUP) was calculated for each gene to estimate the frequency of codon  
418 usage for different amino acids as described previously (Patil & Sonti, 2004), using “The  
419 Sequence Manipulation Suite” webtool (Stothard, 2000). Briefly, eight amino acids (Glycine,  
420 Valine, Threonine, Leucine, Arginine, Serine, Proline and Alanine) were selected, which  
421 have at least four synonymous, and the percentage of codons that end with G or C was  
422 calculated for each amino acid and gene. The first group was chosen to include housekeeping  
423 genes that encode proteins which participate in various essential functions in *Xoo*. These  
424 genes encode: BXO1\_013815 (TonB-dependent siderophore receptor), BXO1\_013910  
425 (*Xanthomonas* adhesin like protein), BXO1\_006505 (*rpfF*), BXO1\_016165 (shikimate  
426 dehydrogenase) and BXO1\_019245 (secreted xylanase). The LPS cluster, which was earlier  
427 shown to have come in *Xoo* by horizontal gene transfer (Patil & Sonti, 2004), was taken as a  
428 control group. This group consisted of five genes of the LPS cluster: BXO1\_014260 (*smtA*),  
429 BXO1\_014255 (*wxoA*), BXO1\_014250 (*wxoB*), BXO1\_014240 (*wxoC*) and BXO1\_014235  
430 (*wxoD*).

## 431 **Western blotting**

432 Bacterial cultures were grown to saturation, pelleted and analysed for the presence of XopQ  
433 protein. Cells were lysed by sonication and total protein supernatants were isolated after  
434 centrifugation at 14,000 rpm for 15 min at 4 °C to remove cellular debris. Equal amounts of  
435 isolated protein supernatants were further used for Western blotting. The XopQ protein was  
436 detected using anti-XopQ antibodies raised in rabbit. Immunoblotting was carried out using  
437 ALP conjugated to anti-rabbit immunoglobulin G secondary antibody (Sigma Aldrich;  
438 A3687). Equal loading of protein in the different samples was shown using Coomassie blue  
439 staining of gels.

#### 440 **Global transcriptome analysis using RNA-seq**

441 Total RNA was sequenced at the NGC facility of CDFD, Hyderabad, with RNA isolated  
442 from the cell pellets of *Xoo* strains (BXO43 and *xopQ*-) grown to an O.D.<sub>600</sub>=1 in PS media.  
443 Quality of the RNA was checked on Agilent TapeStation 4200. Ribosomal RNA (rRNA)  
444 depletion was carried out using the NEBNext® rRNA Depletion Kit (Bacteria), and library  
445 preparation was carried out using NEBNext® Ultra™ II Directional RNA Library Prep Kit  
446 for Illumina®. Prepared libraries were sequenced on Illumina Nextseq2000 (P2 200 cycle  
447 sequencing kit) to generate 60M, 2x100bp reads/sample. The sequenced data was processed  
448 to generate FASTQ files. Differential gene expression analysis was conducted on the  
449 generated data using STAR-featureCounts-DEseq2 pipeline. A false discovery rate (FDR) ≤  
450 0.05, and  $|\log_2$  of the fold changes| ≥1 was considered for differentially expressed genes.  
451 Gene Ontology enrichment analyses were performed with PANTHER using the Gene  
452 Ontology Resource (2021, Ashburner, Ball et al., 2000, Mi, Muruganujan et al., 2019) and  
453 the pathway analyses were performed using KEGG database.

#### 454 **RNA isolation and gene expression analysis**

455 For RNA isolation, bacterial cultures were grown to  $O.D._{600} = 1$ , pelleted and RNA was  
456 extracted using Macherey-Nagel RNA isolation kit according to the manufacturer's  
457 instructions, which included on-column digestion of genomic DNA. 5  $\mu$ g of total RNA was  
458 reverse transcribed into cDNA using EcoDry™ Premix (Clontech, Mountain View, CA,  
459 USA) according to the manufacturer's instructions using random hexamer primers.  
460 Synthesized cDNA was diluted 5-fold and then used for semi-quantitative RT-PCR with 35  
461 cycles of amplification. 16S rRNA was used as an internal control. The cDNA was analysed  
462 for the presence of *xopQ* (600 bp N-terminal fragment) and *ipt* (750 bp full-length gene)  
463 transcripts. Absence of genomic DNA was confirmed using a set of primers from a non-  
464 coding unique region of the genomic DNA.

465 Transcript analysis of genes found to be differentially expressed by RNA-seq in the *xopQ*-  
466 mutant as compared to BXO43, was carried out by reverse transcriptase-quantitative  
467 polymerase chain reaction (RT-qPCR). RT-qPCR of selected genes (Appendix Table S4) was  
468 performed using gene-specific primers using Power SYBR Green PCR Master Mix (Thermo  
469 Fisher Scientific) in BioRad CFX384 Real-Time PCR System (Hercules, California, United  
470 States). Relative expression was calculated with respect to BXO43. The fold change was  
471 calculated using  $2^{-\Delta\Delta Ct}$  method (Livak & Schmittgen, 2001). Expression of 16S rRNA gene  
472 was used as internal control.

### 473 **Bioinformatic analysis of IPT protein**

474 Multiple sequence alignment of the IPT protein from various bacterial strains was carried out  
475 using T-Coffee multiple sequence alignment server (Expresso) (Notredame, Higgins et al.,  
476 2000). The GenBank ID of the IPT homologue in *Xanthomonas oryzae* pv. *oryzicola* BLS256  
477 is AEQ96873, in *Xanthomonas oryzae* pv. *oryzae* PXO99A is ACD58327, in *Xanthomonas*  
478 *albilineans* is WP\_012917043, in *Xanthomonas translucens* is WP\_053834798, in

479 *Xanthomonas theicola* is WP\_128421291, in *Agrobacterium rhizogenes* is WP\_080705458,  
480 in *Ralstonia solanacearum* is WP\_119447925, in *Ensifer psoraleae* is WP\_173514402, in  
481 *Agrobacterium vitis* is WP\_070167542, in *Pseudomonas savastanoi* is AGC31315, in  
482 *Pseudomonas amygdali* is WP\_081007393, in *Rhizobium tumorigenes* is WP\_111221635, in  
483 *Sinorhizobium* sp. PC2 is WP\_046120136, in *Agrobacterium tumefaciens* is QTG17184 and  
484 in *Pseudomonas psychrotolerans* is WP\_193755078.

485 For phylogenetic analysis of the IPT protein, a phylogenetic tree was constructed based on  
486 the sequence of IPT proteins from bacteria, plants, fungi, and Archaea using the MEGA X  
487 software (Kumar, Stecher et al., 2018). Briefly, iterative searching for IPT protein was  
488 performed using position-specific iterated BLAST (PSI-BLAST) method in NCBI (National  
489 Centre for Biotechnology Information) (Altschul, Madden et al., 1997). Phylogenetic tree  
490 analyses was conducted in MEGA X software using Maximum Likelihood method based on  
491 Le Gascuel 2008 model (Le & Gascuel, 2008). The tree with the highest log likelihood (-  
492 56444.14) is shown.

493

#### 494 **References:**

495 (2021) The Gene Ontology resource: enriching a GOld mine. *Nucleic acids research* 49: D325-d334  
496 Altschul SF, Madden TL, Schäffer AA, Zhang J, Zhang Z, Miller W, Lipman DJ (1997) Gapped BLAST  
497 and PSI-BLAST: a new generation of protein database search programs. *Nucleic acids research* 25:  
498 3389-402  
499 Ashburner M, Ball CA, Blake JA, Botstein D, Butler H, Cherry JM, Davis AP, Dolinski K, Dwight SS,  
500 Eppig JT, Harris MA, Hill DP, Issel-Tarver L, Kasarskis A, Lewis S, Matese JC, Richardson JE, Ringwald  
501 M, Rubin GM, Sherlock G (2000) Gene ontology: tool for the unification of biology. *The Gene*  
502 *Ontology Consortium*. *Nature genetics* 25: 25-9  
503 Cenens W, Andrade MO, Llontop E, Alvarez-Martinez CE, Sgro GG, Farah CS (2020) Bactericidal type  
504 IV secretion system homeostasis in *Xanthomonas citri*. *PLoS pathogens* 16: e1008561  
505 Deb S, Ghosh P, Patel HK, Sonti RV (2020) Interaction of the *Xanthomonas* effectors XopQ and XopX  
506 results in induction of rice immune responses. *The Plant journal : for cell and molecular biology*  
507 Deb S, Gupta MK, Patel HK, Sonti RV (2019) *Xanthomonas oryzae* pv. *oryzae* XopQ protein  
508 suppresses rice immune responses through interaction with two 14-3-3 proteins but its phospho-null  
509 mutant induces rice immune responses and interacts with another 14-3-3 protein. *Molecular plant*  
510 *pathology*

511 Elhenawy W, Hordienko S, Gould S, Oberc AM, Tsai CN, Hubbard TP, Waldor MK, Coombes BK (2021)  
512 High-throughput fitness screening and transcriptomics identify a role for a type IV secretion system  
513 in the pathogenesis of Crohn's disease-associated *Escherichia coli*. *Nature communications* 12: 2032  
514 Frébortová J, Greplová M, Seidl MF, Heyl A, Frébort I (2015) Biochemical Characterization of Putative  
515 Adenylate Dimethylallyltransferase and Cytokinin Dehydrogenase from *Nostoc* sp. PCC 7120. *PLoS*  
516 *one* 10: e0138468-e0138468  
517 Giska F, Lichocka M, Piechocki M, Dadlez M, Schmelzer E, Hennig J, Krzymowska M (2013)  
518 Phosphorylation of HopQ1, a type III effector from *Pseudomonas syringae*, creates a binding site for  
519 host 14-3-3 proteins. *Plant physiology* 161: 2049-61  
520 Großkinsky DK, Tafner R, Moreno MV, Stenglein SA, García de Salamone IE, Nelson LM, Novák O,  
521 Strnad M, van der Graaff E, Roitsch T (2016) Cytokinin production by *Pseudomonas fluorescens* G20-  
522 18 determines biocontrol activity against *Pseudomonas syringae* in *Arabidopsis*. *Scientific reports* 6:  
523 23310  
524 Gupta MK, Nathawat R, Sinha D, Haque AS, Sankaranarayanan R, Sonti RV (2015) Mutations in the  
525 Predicted Active Site of *Xanthomonas oryzae* pv. *oryzae* XopQ Differentially Affect Virulence,  
526 Suppression of Host Innate Immunity, and Induction of the HR in a Nonhost Plant. *Molecular plant-*  
527 *microbe interactions* : *MPMI* 28: 195-206  
528 Hann DR, Dominguez-Ferreras A, Motyka V, Dobrev PI, Schornack S, Jehle A, Felix G, Chinchilla D,  
529 Rathjen JP, Boller T (2014) The *Pseudomonas* type III effector HopQ1 activates cytokinin signaling  
530 and interferes with plant innate immunity. *The New phytologist* 201: 585-98  
531 Huang L, Wang L, Lin X, Su Y, Qin Y, Kong W, Zhao L, Xu X, Yan Q (2017) *mcp*, *aer*, *cheB*, and *cheV*  
532 contribute to the regulation of *Vibrio alginolyticus* (ND-01) adhesion under gradients of  
533 environmental factors. *MicrobiologyOpen* 6: e00517  
534 Kuchma SL, Connolly JP, O'Toole GA (2005) A three-component regulatory system regulates biofilm  
535 maturation and type III secretion in *Pseudomonas aeruginosa*. *Journal of bacteriology* 187: 1441-54  
536 Kumar S, Stecher G, Li M, Knyaz C, Tamura K (2018) MEGA X: Molecular Evolutionary Genetics  
537 Analysis across Computing Platforms. *Molecular biology and evolution* 35: 1547-1549  
538 Kurakawa T, Ueda N, Maekawa M, Kobayashi K, Kojima M, Nagato Y, Sakakibara H, Kyojuka J (2007)  
539 Direct control of shoot meristem activity by a cytokinin-activating enzyme. *Nature* 445: 652-5  
540 Le SQ, Gascuel O (2008) An improved general amino acid replacement matrix. *Molecular biology and*  
541 *evolution* 25: 1307-20  
542 Li W, Chiang YH, Coaker G (2013) The HopQ1 effector's nucleoside hydrolase-like domain is required  
543 for bacterial virulence in *Arabidopsis* and tomato, but not host recognition in tobacco. *PLoS one* 8:  
544 e59684  
545 Li W, Yadeta KA, Elmore JM, Coaker G (2013) The *Pseudomonas syringae* effector HopQ1 promotes  
546 bacterial virulence and interacts with tomato 14-3-3 proteins in a phosphorylation-dependent  
547 manner. *Plant physiology* 161: 2062-74  
548 Livak KJ, Schmittgen TD (2001) Analysis of relative gene expression data using real-time quantitative  
549 PCR and the 2<sup>-ΔΔC<sub>T</sub></sup> Method. *Methods (San Diego, Calif)* 25: 402-8  
550 Mi H, Muruganujan A, Ebert D, Huang X, Thomas PD (2019) PANTHER version 14: more genomes, a  
551 new PANTHER GO-slim and improvements in enrichment analysis tools. *Nucleic acids research* 47:  
552 D419-d426  
553 Midha S, Bansal K, Kumar S, Girija AM, Mishra D, Brahma K, Laha GS, Sundaram RM, Sonti RV, Patil  
554 PB (2017) Population genomic insights into variation and evolution of *Xanthomonas oryzae* pv.  
555 *oryzae*. *Scientific reports* 7: 40694-40694  
556 Nayar S (2021) Exploring the Role of a Cytokinin-Activating Enzyme LONELY GUY in Unicellular  
557 Microalga *Chlorella variabilis*. *Frontiers in plant science* 11  
558 Notredame C, Higgins DG, Heringa J (2000) T-Coffee: A novel method for fast and accurate multiple  
559 sequence alignment. *Journal of molecular biology* 302: 205-17  
560 Osugi A, Sakakibara H (2015) Q&A: How do plants respond to cytokinins and what is their  
561 importance? *BMC biology* 13: 102

562 Patil PB, Sonti RV (2004) Variation suggestive of horizontal gene transfer at a lipopolysaccharide (lps)  
563 biosynthetic locus in *Xanthomonas oryzae* pv. *oryzae*, the bacterial leaf blight pathogen of rice. *BMC*  
564 *microbiology* 4: 40  
565 Pertry I, Václavíková K, Depuydt S, Galuszka P, Spíchal L, Temmerman W, Stes E, Schmölling T,  
566 Kakimoto T, Van Montagu MCE, Strnad M, Holsters M, Tarkowski P, Vereecke D (2009) Identification  
567 of *Rhodococcus fascians* cytokinins and their modus operandi to reshape the plant.  
568 *Proceedings of the National Academy of Sciences* 106: 929-934  
569 Qi Y-H, Huang L, Liu G-F, Leng M, Lu G-T (2020) PilG and PilH antagonistically control flagellum-  
570 dependent and pili-dependent motility in the phytopathogen *Xanthomonas campestris* pv.  
571 *campestris*. *BMC microbiology* 20: 37  
572 Samanovic MI, Tu S, Novák O, Iyer LM, McAllister FE, Aravind L, Gygi SP, Hubbard SR, Strnad M,  
573 Darwin KH (2015) Proteasomal control of cytokinin synthesis protects *Mycobacterium tuberculosis*  
574 against nitric oxide. *Molecular cell* 57: 984-994  
575 Sardesai N, Lee L-Y, Chen H, Yi H, Olbricht GR, Stirnberg A, Jeffries J, Xiong K, Doerge RW, Gelvin SB  
576 (2013) Cytokinins Secreted by *Agrobacterium* Promote Transformation by Repressing a  
577 Plant Myb Transcription Factor. *Science Signaling* 6: ra100-ra100  
578 Seifert HS (2017) *Haemophilus* spills its guts to make a biofilm. *Proceedings of the National Academy*  
579 *of Sciences of the United States of America* 114: 8444-8446  
580 Seo H, Kim K-J (2017) Structural basis for a novel type of cytokinin-activating protein. *Scientific*  
581 *reports* 7: 45985-45985  
582 Stothard P (2000) The sequence manipulation suite: JavaScript programs for analyzing and  
583 formatting protein and DNA sequences. *BioTechniques* 28: 1102, 1104  
584 Stuurman N, Pacios Bras C, Schlaman HR, Wijffjes AH, Bloemberg G, Spaink HP (2000) Use of green  
585 fluorescent protein color variants expressed on stable broad-host-range vectors to visualize rhizobia  
586 interacting with plants. *Molecular plant-microbe interactions : MPMI* 13: 1163-9  
587 Teper D, Salomon D, Sunitha S, Kim JG, Mudgett MB, Sessa G (2014) *Xanthomonas euvesicatoria*  
588 type III effector XopQ interacts with tomato and pepper 14-3-3 isoforms to suppress effector-  
589 triggered immunity. *The Plant journal : for cell and molecular biology* 77: 297-309  
590 Wang FF, Cheng ST, Wu Y, Ren BZ, Qian W (2017) A Bacterial Receptor PcrK Senses the Plant  
591 Hormone Cytokinin to Promote Adaptation to Oxidative Stress. *Cell Rep* 21: 2940-2951

592

## 593 **Figure Legends:**

594 **Figure 1. The XopQ protein is a phosphoribose-hydrolase which produces and secretes**  
595 **cytokinin for the planktonic growth of *X. oryzae* pv. *oryzae*. A-D, Cytokinin estimation**  
596 **was carried out from the bacterial cell pellets and culture supernatant by LC-MS using the**  
597 **different *Xoo* strains. Isopentenyl adenine (iP) (A, B) and trans- zeatin (tZ) (C, D) was**  
598 **measured in cell pellet and culture supernatant. Values are presented as nanogram of**  
599 **cytokinin per gram of dry weight of lyophilised sample  $\pm$  standard deviation from 3**  
600 **biological replicates. E, Microscopy images of the different *Xoo* strains. Images were**  
601 **acquired at 100X in DIC (Nomarski). Scale bar represents 5  $\mu$ m. F-H. Cell attachment and**

602 static biofilm assay of *Xoo* strains. **G**, Quantification of bacterial cells in the cell suspension.  
603 Values are presented as mean absorbance (at 600 nm)  $\pm$  standard deviation from 5 replicates.  
604 **H**, Quantification of bacterial cells attached to glass tubes by staining with crystal violet.  
605 Values are presented as mean absorbance (at 570 nm)  $\pm$  standard deviation from 5 replicates.  
606 **I- J**, Surface visualisation of biofilm formed by the BXO43/EGFP and *xopQ*-/EGFP strains.  
607 Scale bar represents 15  $\mu$ m. Thickness of the biofilm is presented as mean  $\pm$  standard  
608 deviation from 5 replicates. Asterisk indicates significant difference ( $P= 0.0197$ ) in  
609 comparison with the BXO43 strain. (**J**). For all graphs, columns/boxes capped with letters  
610 that are different from one another indicate that they are statistically different using unpaired  
611 two- sided Student's t-test analysis ( $P \leq 0.05$ ). Images are representative of 3 biological  
612 replicates (**E, F, I**).

613 **Figure 2. Supplementation with exogenous cytokinin converts a *xopQ*- mutant from**  
614 **biofilm to planktonic lifestyle and restores wildtype levels of virulence. A**, Microscopy  
615 analysis was performed of the *Xoo* strains, with and without the addition of iP. Images were  
616 acquired at 100X in DIC (Nomarski). Scale bar represents 5  $\mu$ m. **B-D**. Cell attachment and  
617 static biofilm assay was performed of the *Xoo* strains, with and without the addition of iP. **C**,  
618 Quantification of bacterial cells in the cell suspension. Values are presented as mean  
619 absorbance (at 600 nm)  $\pm$  standard deviation from 5 replicates. **D**, Quantification of bacterial  
620 cells attached to glass tubes by staining with crystal violet. Values are presented as mean  
621 absorbance (at 570 nm)  $\pm$  standard deviation from 5 replicates. **E- F**, Surface visualisation of  
622 biofilm formed by the BXO43/EGFP and *xopQ*-/EGFP strains, with and without the addition  
623 of iP. Scale bar represents 15 $\mu$ m. **F**, Thickness of the biofilm is presented as mean  $\pm$  standard  
624 deviation from 5 replicates. **G**, Co- culturing of wildtype *Xoo* BXO43 with the *xopQ*- mutant  
625 reverses biofilm to planktonic lifestyle of *Xoo*. Microscopy analysis was performed of the  
626 BXO43/mCherry and *xopQ*-/EGFP strains, either singly, or following co- culturing for 4 h at



627 28 °C. Images were acquired at 100X for fluorescence channels and DIC (Nomarski). Scale  
628 bar represents 5 µm. **H**, Supplementation with exogenous cytokinin restores wildtype levels  
629 of virulence to a *xopQ*- mutant of *Xoo*. Rice leaves were inoculated by pin- pricking with the  
630 various *Xoo* strains, with and without prior midvein injection of iP. Lesion lengths were  
631 measured 14 days after inoculation. Error bars indicate the standard deviation of readings  
632 from 5 inoculated leaves. For all graphs, boxes capped with letters that are different from one  
633 another indicate that they are statistically different using unpaired two- sided Student's t-test  
634 analysis ( $P \leq 0.05$ ). Images are representative of 3 biological replicates (**A**, **B**, **E**, **G**).

635 **Figure 3. The isopentenyl transferase gene is required for planktonic lifestyle and full**  
636 **virulence of *Xoo*.** **A**, Schematic of open reading frames (ORF) based on sequence of 4777 bp  
637 genomic region encompassing the IPT locus of the *Xoo* BXO1 strain. Arrows represent the  
638 ORF and direction of transcription. The predicted ORFs upstream of *ipt* gene encode a  
639 hypothetical protein, an endolysin, an IS630 transposase and a lysozyme. The predicted  
640 ORFs downstream of *ipt* gene in BXO1 exhibit high similarity to a DNA helicase and a helix-  
641 turn-helix protein. ORFs marked in green represent the 4777 bp region present in *Xoo* but not  
642 in *Xcv* or *Xcc*. ORFs marked in pink denote the flanking genes, conserved in *Xcv* and *Xcc* **B**,  
643 GC content of IPT locus. **C**, Codon usage pattern of *ipt* gene, HK (housekeeping) genes and  
644 LPS cluster **D**, Codon usage pattern of *ipt* gene cluster (excluding IS630 transposase), HK  
645 genes and LPS cluster **e**, Microscopy analysis was performed of the *Xoo* strains. Images were  
646 acquired at 100X in DIC (Nomarski). Scale bar represents 5 µm. **F-H**, Cell attachment and  
647 static biofilm assay of *Xoo* strains BXO43, *ipt*-, *ipt*-/pHM1 or *ipt*-/pHM1::*ipt*. **G**,  
648 Quantification of bacterial cells in the cell suspension. Values are presented as mean  
649 absorbance (at 600 nm) ± standard deviation from 5 replicates. **H**, Quantification of bacterial  
650 cells attached to glass tubes by staining with crystal violet. Values are presented as mean  
651 absorbance (at 570 nm) ± standard deviation from 5 replicates. **I-J**, Surface visualisation of

652 biofilm formed by the BXO43/EGFP and *ipt*-/EGFP strains. Scale bar represents 15  $\mu$ m. **J**,  
653 Thickness of the biofilm is presented as mean  $\pm$  standard deviation from 5 replicates. Asterisk  
654 indicates significant difference ( $P= 0.0209$ ) in comparison with the BXO43 strain. **K-N**,  
655 Cytokinin estimation was carried out from the bacterial cell pellets and culture supernatant of  
656 *Xoo* strains by LC-MS. iP (**K, L**) and tZ (**M, N**) was measured in cell pellet and culture  
657 supernatant. Values are presented as nanogram of cytokinin per gram of dry weight of  
658 lyophilised sample  $\pm$  standard deviation from 3 biological replicates. **O-P**, A *ipt*- mutant of  
659 BXO43 is virulence deficient. Leaves of susceptible rice TN-1 were clip inoculated with  
660 different *Xoo* strains. **O**, Lesion lengths were measured 14 days after inoculation. Error bars  
661 indicate the standard deviation of readings from 5 inoculated leaves. **P**, Virulence phenotype  
662 on rice leaves. Leaves were photographed 14 days after inoculation. For all graphs,  
663 columns/boxes capped with letters that are different from one another indicate that they are  
664 statistically different using unpaired two- sided Student's t-test analysis ( $P \leq 0.05$ ). Images  
665 are representative of 3 biological replicates (**E, F, I, P**).

666 **Figure 4. Supplementation of *ipt*- with active cytokinin reverses biofilm to planktonic**  
667 **lifestyle and restores wildtype levels of virulence. A**, Microscopy analysis was performed  
668 of the following strains: BXO43, *ipt*- or *ipt*- + iP. Images were acquired at 100X in DIC  
669 (Nomarski). Scale bar represents 5 $\mu$ m. **B-D**. Cell attachment and static biofilm assay of *Xoo*  
670 strains BXO43, *ipt*- or *ipt*- + iP. **c**, Quantification of bacterial cells in the cell suspension.  
671 Values are presented as mean absorbance (at 600 nm)  $\pm$  standard deviation from 5 replicates.  
672 **D**, Quantification of bacterial cells attached to glass tubes by staining with crystal violet.  
673 Values are presented as mean absorbance (at 570 nm)  $\pm$  standard deviation from 5 replicates.  
674 **E- F**, Surface visualisation of biofilm formed by the BXO43/EGFP and *ipt*-/EGFP strains.  
675 Scale bar represents 15  $\mu$ m. **F**, Thickness of the biofilm is presented as mean  $\pm$  standard  
676 deviation from 5 replicates. **G**, Co- culturing of wildtype *Xoo* BXO43 with the *ipt*- mutant

677 reverses biofilm to planktonic lifestyle of *Xoo*. Microscopy analysis was performed of the  
678 BXO43/mCherry and *ipt*-EGFP strains, either singly, or following co- culturing for 4 h at 28  
679 °C. Images were acquired at 100X for fluorescence channels and DIC (Nomarski). Scale bar  
680 represents 5 μm. **H**, Supplementation with exogenous cytokinin restores wildtype levels of  
681 virulence to a *ipt*- mutant of *Xoo*. TN-1 rice leaves were inoculated with BXO43, *ipt*-, or *ipt*-  
682 with injection of iP, 24 h prior to infection with *ipt*-. Lesion lengths were measured 14 days  
683 after inoculation. Error bars indicate the standard deviation of readings from 5 inoculated  
684 leaves. For all graphs, boxes capped with letters that are different from one another indicate  
685 that they are statistically different using unpaired two- sided Student's t-test analysis ( $P \leq$   
686 0.05). Images are representative of 3 biological replicates (**A**, **B**, **E**, **G**).

687 **Figure 5. The *pcrK/pcrR* genes are required for cytokinin sensing and virulence in *Xoo*.**

688 **A**, Microscopy analysis was performed of the following strains: BXO43, *pcrK*- or *pcrR*-.  
689 Images were acquired at 100X in DIC (Nomarski). Scale bar represents 5μm. **B-D**. Cell  
690 attachment and static biofilm assay of *Xoo* strains BXO43, *pcrK*- or *pcrR*-. **C**, Quantification  
691 of bacterial cells in the cell suspension. Values are presented as mean absorbance (at 600 nm)  
692 ± standard deviation from 5 replicates. **D**, Quantification of bacterial cells attached to glass  
693 tubes by staining with crystal violet. Values are presented as mean absorbance (at 570 nm) ±  
694 standard deviation from 5 replicates. **E**, Microscopy analysis was performed of the following  
695 strains: BXO43, *pcrK*-, *pcrR*-, *pcrK*- + iP or *pcrR*- + iP. Images were acquired at 100X in  
696 DIC (Nomarski). Scale bar represents 5μm. **F-I**. Cell attachment and static biofilm assay of  
697 *Xoo* strains BXO43, *pcrK*-, *pcrR*-, *pcrK*- + iP or *pcrR*- + iP. **H**, Quantification of bacterial  
698 cells in the cell suspension. Values are presented as mean absorbance (at 600 nm) ± standard  
699 deviation from 5 replicates. **I**, Quantification of bacterial cells attached to glass tubes by  
700 staining with crystal violet. Values are presented as mean absorbance (at 570 nm) ± standard  
701 deviation from 5 replicates. **J**, Co- culturing of wildtype *Xoo* BXO43 with the *pcrK*- or *pcrR*-

702 mutants does not reverse biofilm to planktonic lifestyle of *Xoo*. Microscopy analysis was  
703 performed of the BXO43/mCherry and *pcrK*-EGFP or *pcrR*-EGFP strains, either singly, or  
704 following co- culturing for 4 h at 28 °C. Images were acquired at 100X for fluorescence  
705 channels and DIC (Nomarski). Scale bar represents 5  $\mu\text{m}$ . **K-L**, *pcrK*- and *pcrR*- mutants of  
706 BXO43 are virulence deficient. Leaves of susceptible rice TN-1 were clip inoculated with  
707 different *Xoo* strains. **K**, Lesion lengths were measured 14 days after inoculation. Error bars  
708 indicate the standard deviation of readings from 5 inoculated leaves. **L**, Virulence phenotype  
709 on rice leaves. Leaves were photographed 14 days after inoculation. For all graphs, boxes  
710 capped with letters that are different from one another indicate that they are statistically  
711 different using unpaired two- sided Student's t-test analysis ( $P \leq 0.05$ ). Images are  
712 representative of 3 biological replicates (**B, F, G, J, L**).

713

714

715 **Table 1. The XopQ protein is a phosphoribose-hydrolase which cleaves a cytokinin**  
716 **precursor.** Kinetic parameters of phosphoribose-hydrolase activity of XopQ wildtype and  
717 mutant proteins XopQ D116A and XopQ Y279A of *Xoo*.

Parameters	XopQ	XopQ D116A	XopQ Y279A
$V_{\max}$ ( $\mu\text{M sec}^{-1}$ )	2.84808E-05	2.2531E-05	1.96002E-05
$K_m$ ( $\mu\text{M}$ )	0.191494727	0.174519165	0.180779251
$K_{\text{cat}}$ ( $\text{sec}^{-1}$ )	28.4808237	23.0377589	19.6002059
$K_{\text{cat}}/K_m$ ( $\text{M}^{-1} \text{sec}^{-1}$ )	0.000148729	0.000132007	0.000108421

718

719 **Author Contributions:**

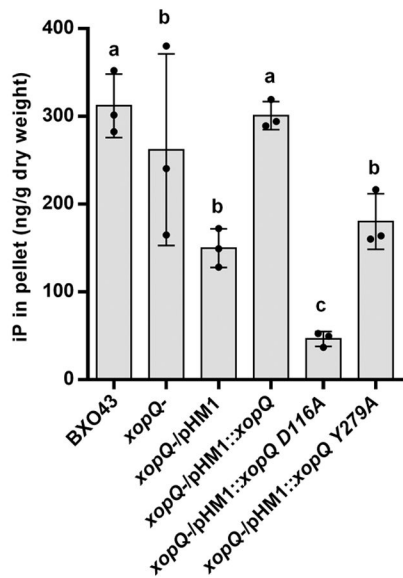
720 SD, HKP and RVS conceived and designed the experiments. SD performed all the biological  
721 assays, and wrote the manuscript. CK and RK performed the cytokinin estimation. AK  
722 performed the genomic bioinformatic analysis. PG assisted in generation of the *pcrK*- and  
723 *pcrR*- mutants. SD, HKP, SC, GJ, PP and RVS analyzed the data, and finalized the  
724 manuscript, which was approved by all the authors. HKP, GJ and RVS contributed  
725 reagents/materials.

726 **Competing interest statement:** The authors declare that no conflict of interest exists.

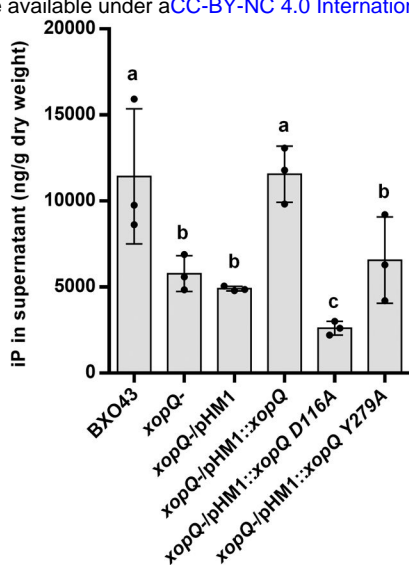
727 **Availability of data and material:** The GEO code for the RNA-sequencing data generated  
728 for this study is GSE179029.

729 **Funding:** This work was supported by grants to HKP from the Council of Scientific and  
730 Industrial Research (CSIR), Government of India. RVS and GJ were supported by the J. C.  
731 Bose Fellowship and the Swarna Jayanti Fellowship, respectively, from the Science and  
732 Engineering Research Board (SERB), Government of India. AK acknowledges CSIR for  
733 fellowship. CK and RK acknowledge the National Institute of Plant Genome Research for  
734 fellowship.

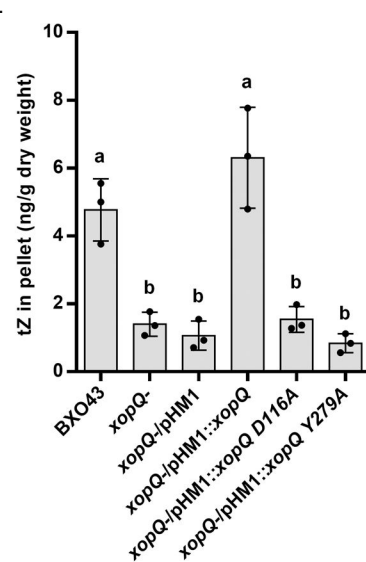
**A**



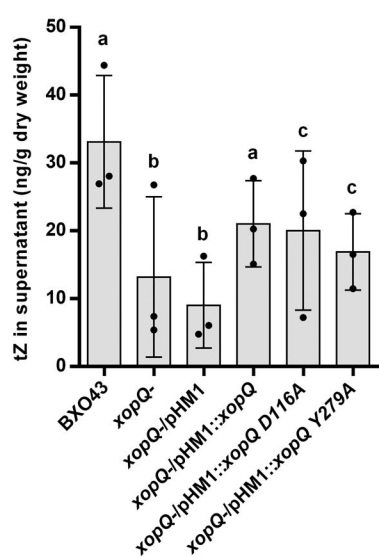
**B**



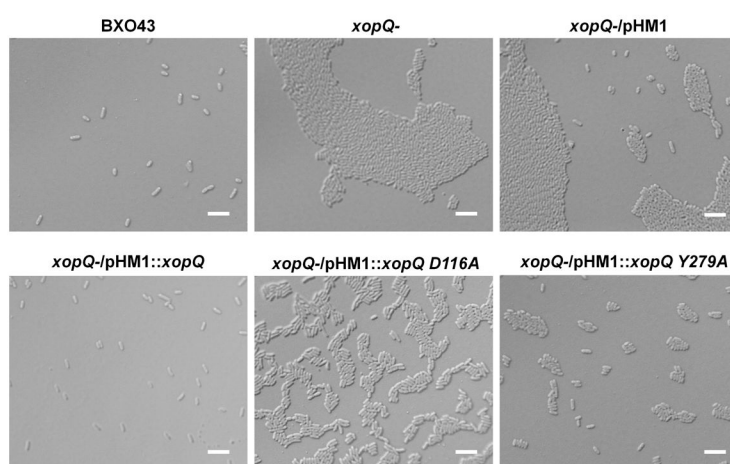
**C**



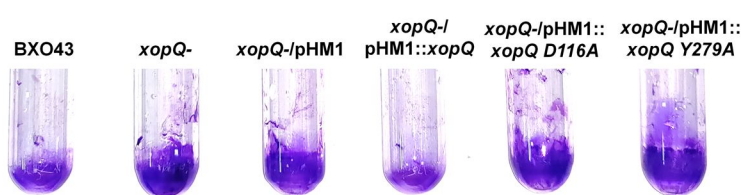
**D**



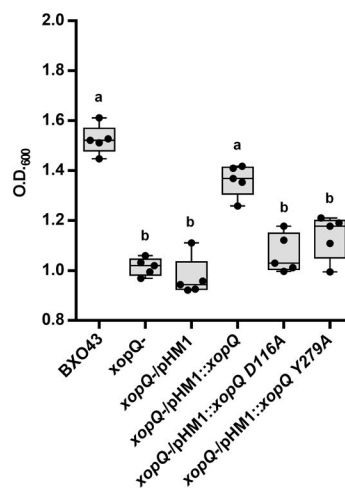
**E**



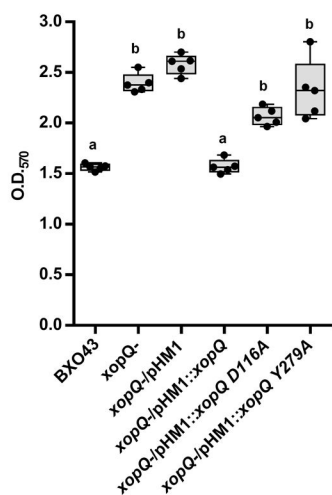
**F**



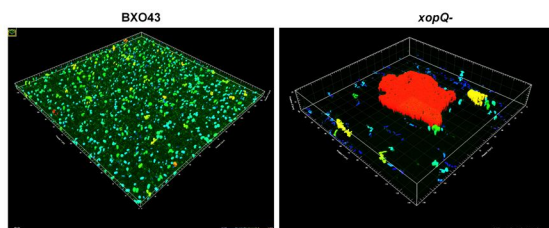
**G**



**H**



**I**



**J**

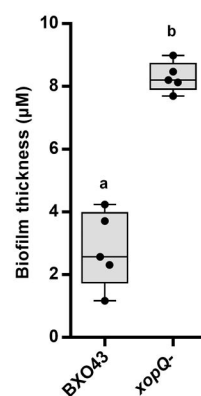
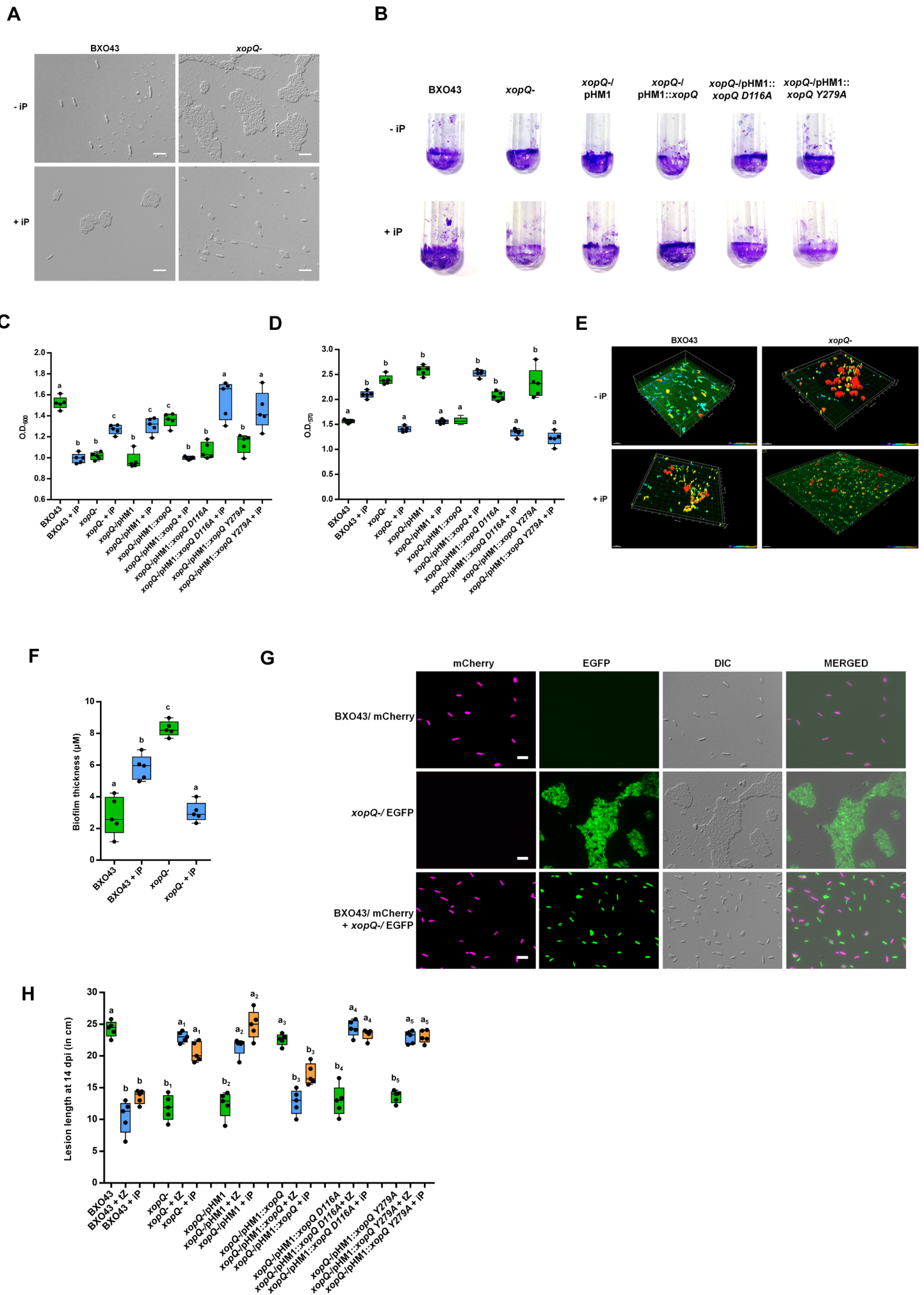
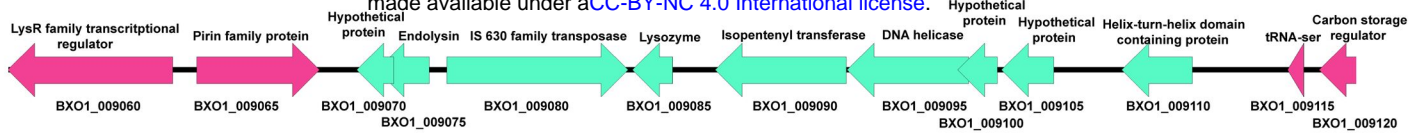


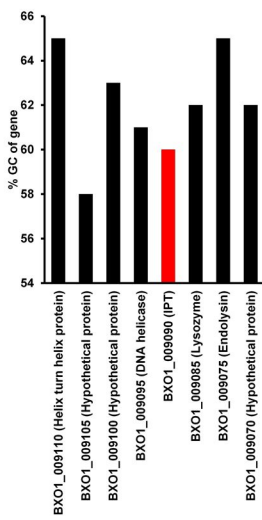
Figure 1



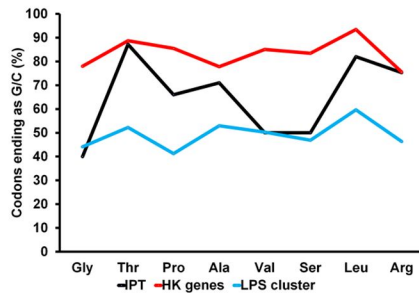
**A**



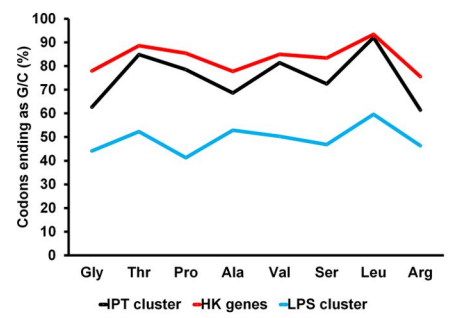
**B**



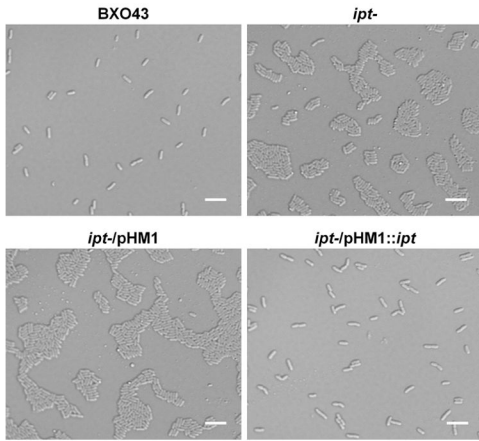
**C**



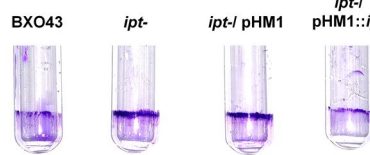
**D**



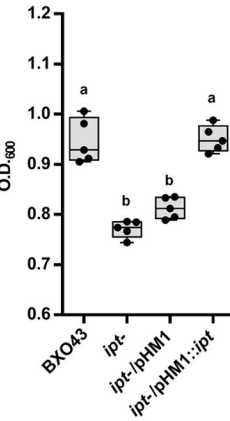
**E**



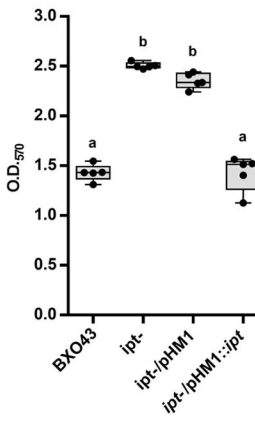
**F**



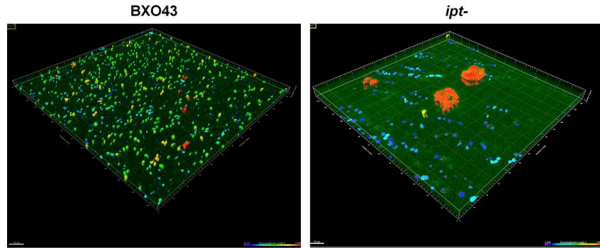
**G**



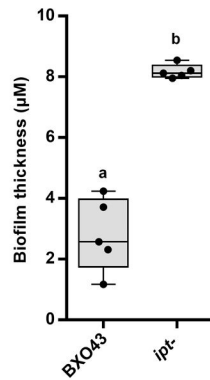
**H**



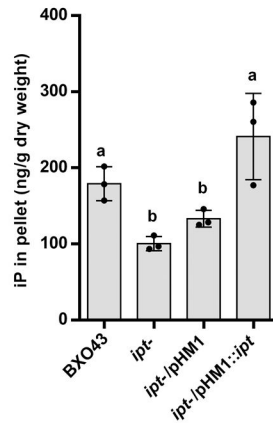
**I**



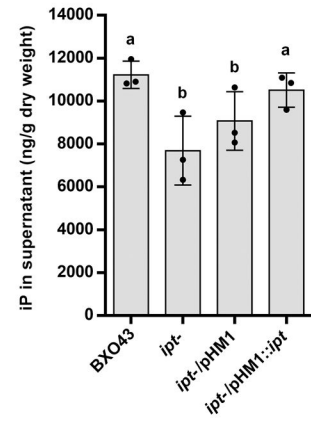
**J**



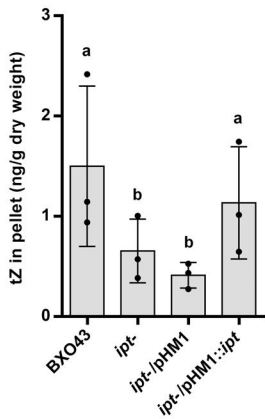
**K**



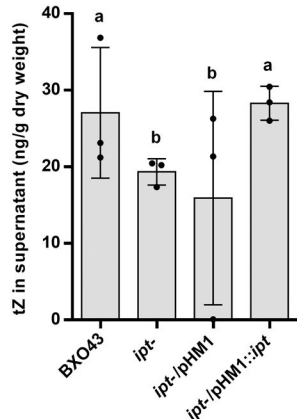
**L**



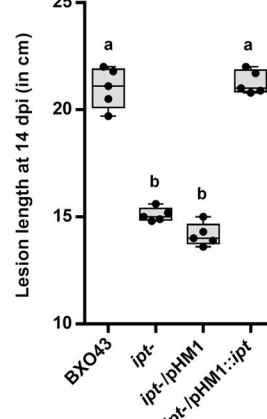
**M**



**N**



**O**



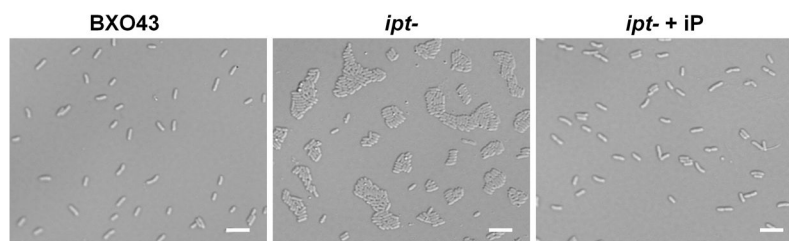
**P**



**Figure 3**



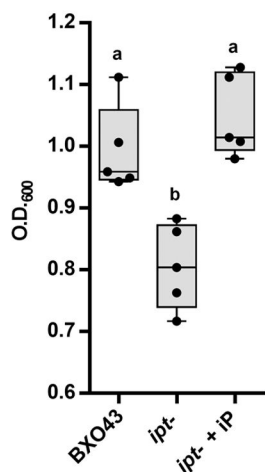
**A**



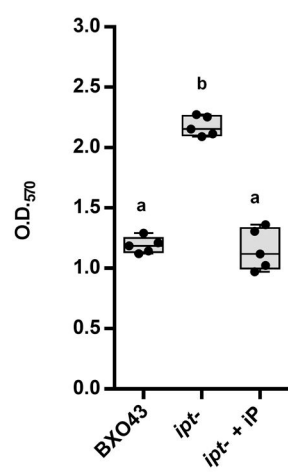
**B**



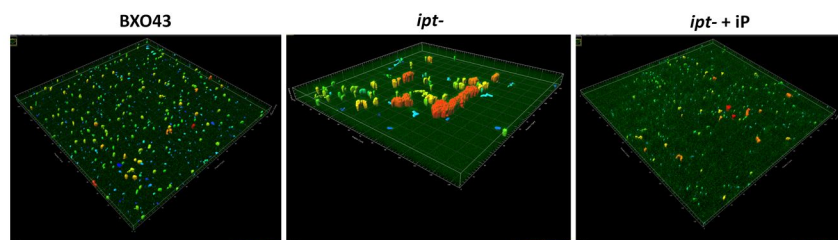
**C**



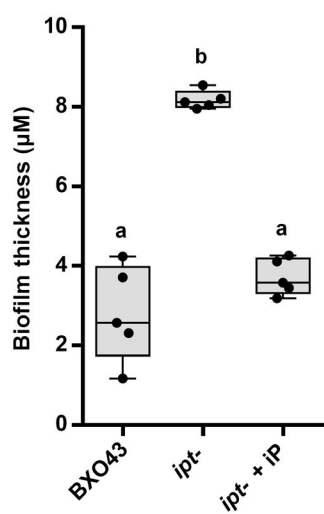
**D**



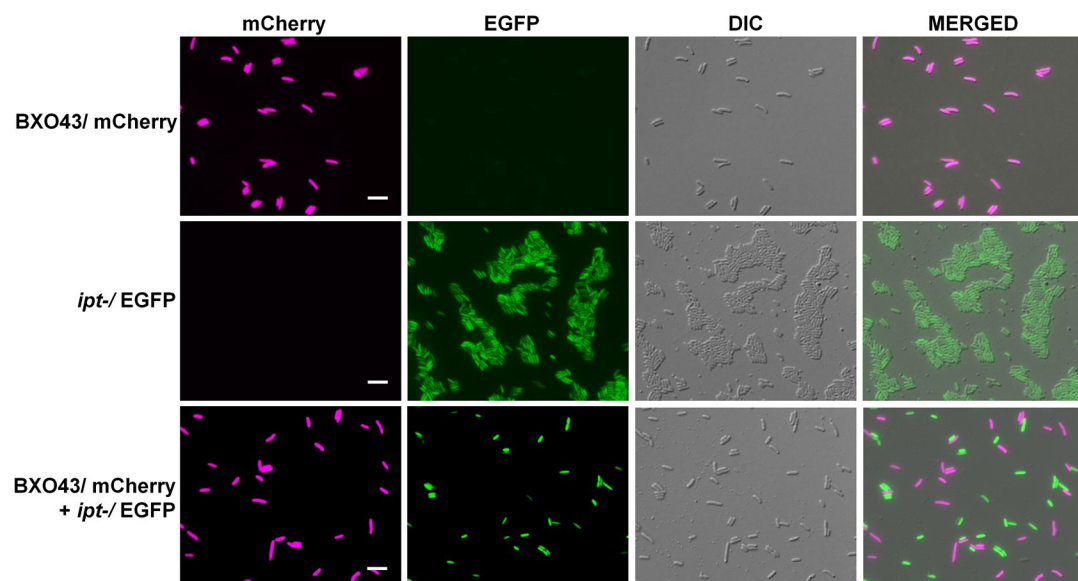
**E**



**F**



**G**



**H**

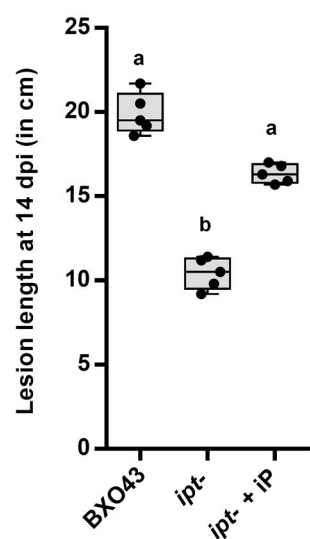
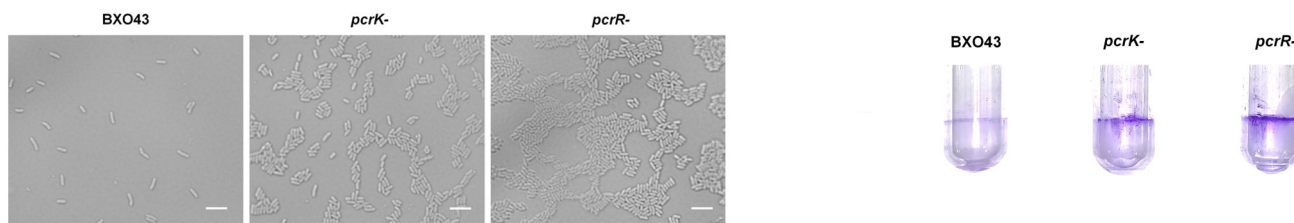
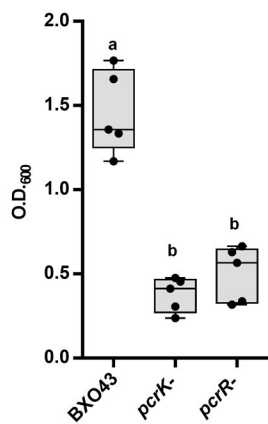


**Figure 4**

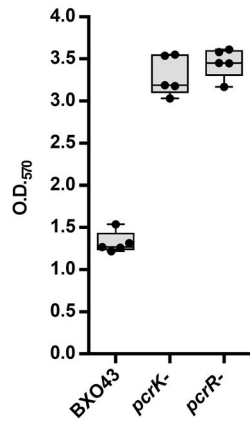
**A**



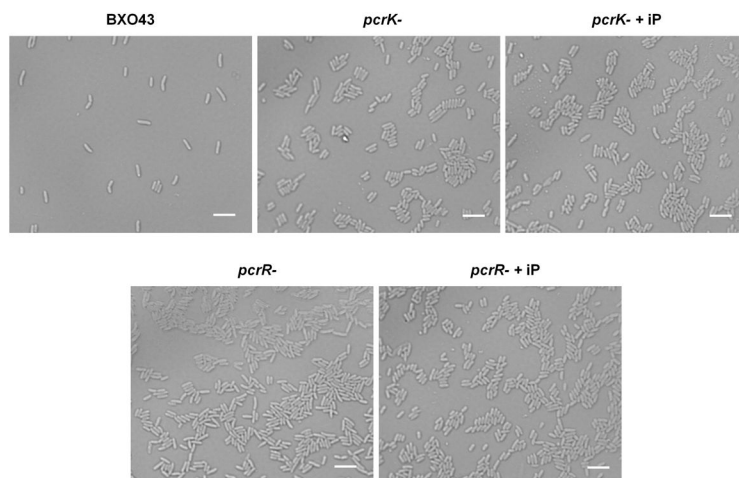
**C**



**D**



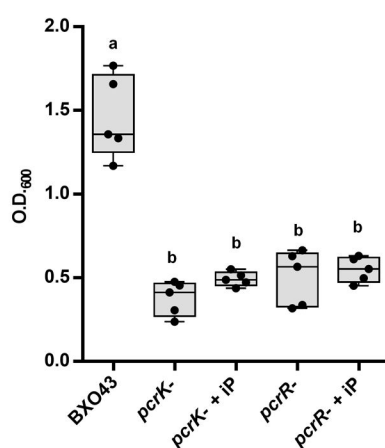
**E**



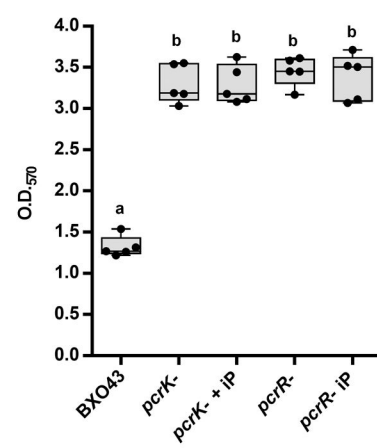
**F**



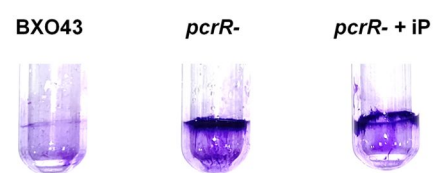
**H**



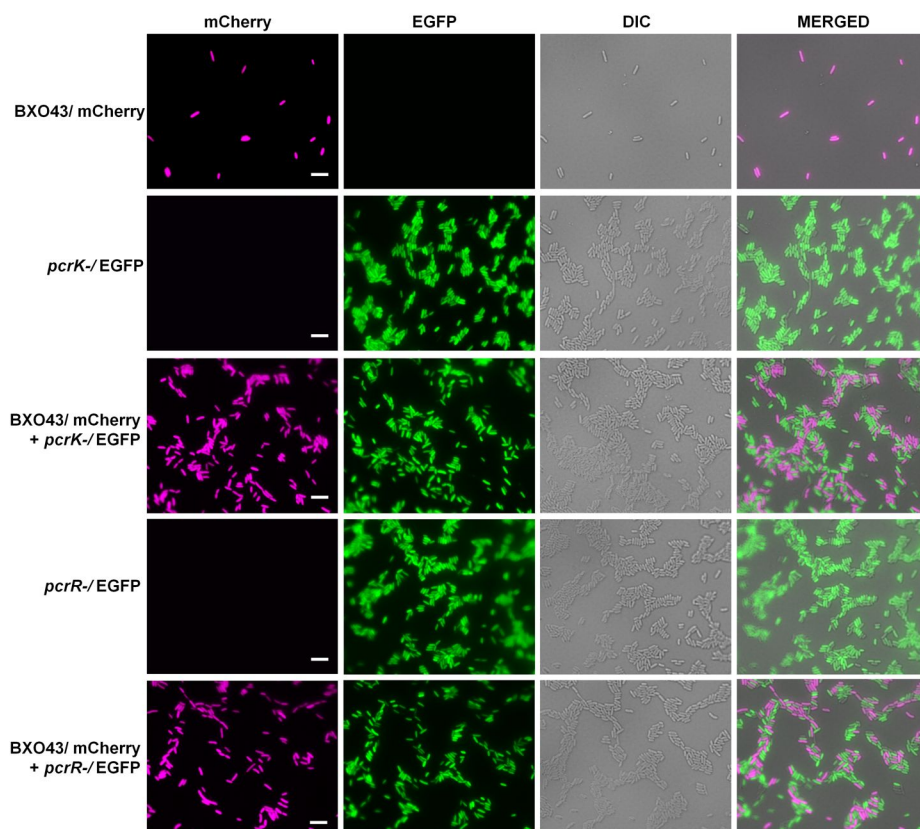
**I**



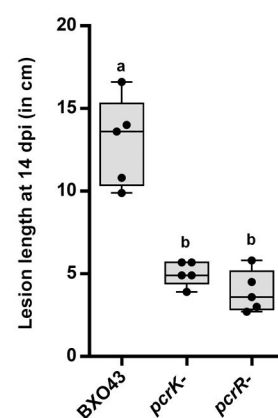
**G**



**J**



**K**



**L**



**Figure 5**